Optik - International Journal for Light and Electron Optics 232 (2021) 166514

Contents lists available at ScienceDirect

Optik

journal homepage: www.elsevier.com/locate/ijleo

Original research article

# A high performance real-time vision system for curved surface inspection

Wang Peng [a,b,*], Jingming Xie [b,*], Zhongkai Gu [c], Qingxi Liao [a], Xuanxuan Huang [a]

[a] *School of Engineering, Huazhong Agricultural University, Wuhan, 430070, China*
[b] *School of Mechanical Science and Engineering, Huazhong University of Science and Technology, Wuhan, 430070, China*
[c] *School of Mechanical Engineering and Automation, Harbin Institute of Technology, HIT Campus Shenzhen University Town, Xili, Shenzhen, 518055, China*

ARTICLE INFO

*Keywords:*
Optical imaging
Curved surface inspection
Vision system
Image processing

ABSTRACT

Surface quality plays an important role in inspection lines. In this paper, a novel imaging device combined with FPGA (Field Programmable Gate Array) based processing platform had been designed to detect and analyse curved surface defects for vision inspection. The optical imaging part was made by an optical device which can be used to collect curved surface features without anamorphose and a camera with 70k Hz linear CMOS was used to capture surface information. The FPGA based inspection platform had been developed for camera control and image processing. Inspecting experiments had been tested with an inspection accuracy of 0.2 mm x 0.2 mm which satisfied a 12 m/s real-time vision inspection line. This research result can be subsequently applied to various surface inspection scenarios.

## 1. Introduction

As a comprehensive technology, vision based automated inspection system has been widely used in industrial areas [1,2], especially in surface quality control, such as wood flooring inspection [3], cigarette packet inspection [4], spalling inspection and quantification in subway networks [5], etc. On automatic detecting lines, vision is used to acquire, detect and sort moving products, and then guide the control system to complete the quality control tasks [6,7]. Machine vision based inspection system is usually configured by two parts: optical imaging device and image processing platform [8–10]. The performance of inspection system mainly depends on the quality of acquired images [11]. Images are affected by two factors: optical illumination system and imaging system [12,13]. In order to capture high quality images, optical illumination system must be configured according to the surface profiles of the objects and specific application. Meanwhile, the imaging system must be reliable to capture the whole surface information without anamorphose.

The existing real-time inspection systems are usually IPC (Industrial Personal Computer)-based instruments, which have the disadvantages of high cost, large space and waste of hardware resources [14,15]. Addressing these issues, incorporating embedded hardware processor into vision system is imperative [16,17]. Compact and high performance embedded vision system is of key importance to automated industry world. When an application requires real-time processing, such as online inspection or real-time trajectory generation of a robotic manipulator [18], the specifications are very strict and easier to implement in embedded

* Corresponding authors at: School of Mechanical Science and Engineering, Huazhong University of Science and Technology, Wuhan, 430070, China.

*E-mail addresses:* pengwang@mail.hzau.edu.cn (W. Peng), xjmhust@hust.edu.cn (J. Xie).

https://doi.org/10.1016/j.ijleo.2021.166514
Received 23 December 2020; Accepted 8 February 2021
Available online 13 February 2021
0030-4026/

hardware. As an embedded chip, FPGA has played a significant role in vision equipment and commercial electronics [19,20]. At the same time, the growing requirement for faster and cost-effective systems triggers a requirement for FPGA, where the inherent parallelism results in better performance [21,22]. In order to realize a high performance real-time inspection system, the FPGA has been selected as the processing platform.

To date, plenty of inspection systems are used to detect flat surface defects, while the curved surface inspection is still a research issue to be solved [23,24]. When project a curved surface directly to a flat detector, the shape of curved part is lost. In order to main the detailed curved surface without losing any valuable information, a curved reflector is created to image the curved surface without anamorphose. High speed real-time optical imaging without distortion is another problem [25–28]. When the speed rate of production lines is very high, it is very difficult to keep original features without distortion or losing the surface profile information [29]. In order to solve this problem, a high frequency line scan CMOS camera is used to capture the curved surface line by line, and the sampling rate of the camera is matched with movement speed of real-time samples.

In this paper, a novel optical device, which is used to acquire curved surface information without anamorphisme, has been simulated and designed. The FPGA based real-time inspection system for curved surfaces is constructed by three parts: sample part, optical system and the FPGA based processing board. The optical device was used to unfold the curved surface into a non-distortion plane image. Then, a camera with 70k Hz linear CMOS was used to capture surface information. The captured image was cached in a flash chip on the FPGA board, and the FPGA was used as a camera control and image processing platform to implement high performance real-time detecting tasks. With parallel computing ability of the FPGA, an embedded, cost-effective curved surface defects inspection instrument will play an important role among vision based inspection applications.

## 2. Materials and methods

### *2.1. Optical device structure*

The optical setup, which can be used to extend the curved surface to plat image without distortion, is unique and delicately designed in this system. The principle of optical structure is shown in Fig. 1(a). Light sources are generated by an LED and propagates into the aperture in glass tube by a reflector. The glass tube is used to keep lens away from contaminants inside the sample. The light interacts with the sample's curved surface in the tube and reflected back on the cylindrical reflector with a certain angle. The reflectors in cylindrical shell are used to extract the surface information on rod sample of glass tube and transmit the related information the light received spot without distortion. After passing through the reflectors in cylindrical shell, the light with curved information is focusing on a light receive spot by a series of lenses. Finally, the texture of curved surface information is obtained by the detector. The inner diameter of glass tube is 8.0 mm. The optical path simulation result is shown in Fig. 1(b). With this setup, the curved surface inside cylindrical tube can be imaged by the reflector attached to the inside surface of tube. Information of the surface can be recorded without losing any details. Then, after passing through a series of related lenses, the original curved surface information focused on the light received spot and received by the detector.

### *2.2. Image acquisition system*

The imaging sensor is DR-2k-7lcc (Awaiba Inc., Portugal), which is a high-speed line scan sampling CMOS (complementary metal-oxide-semiconductor) sensor. The sensor is precisely aligned and perpendicular to the receive spot of optical device. Inside CMOS image sensor, an on-chip analog-to-digital conversion is used to convert analog signals into digital signals which can be used for image processing. As shown in Fig. 2(a), the timing diagram of CMOS sensor is given. The timing sequence is used to activate CMOS sensor by driving the circuits of crystal clock. The SPI (High-speed serial port) has been used as the control part to drive the camera, and CameraLink is used to transfer image data. In order to optimize hardware resource, the FPGA processing board is used to control and

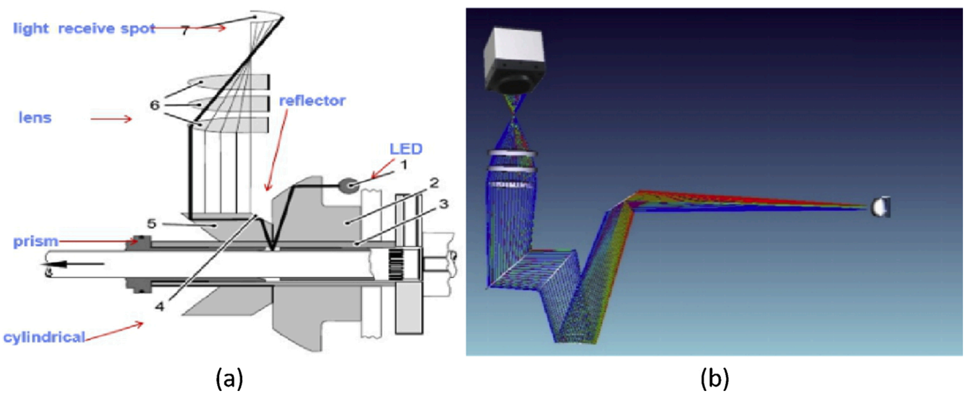


**Fig. 1.** (a) Optical detecting structure: 1-LED, 2-optical transmission component, 3-glass tube, 4-circular mirror, 5-reflector, 6-lenses, 7-light receive spot; (b) Optical path simulation.

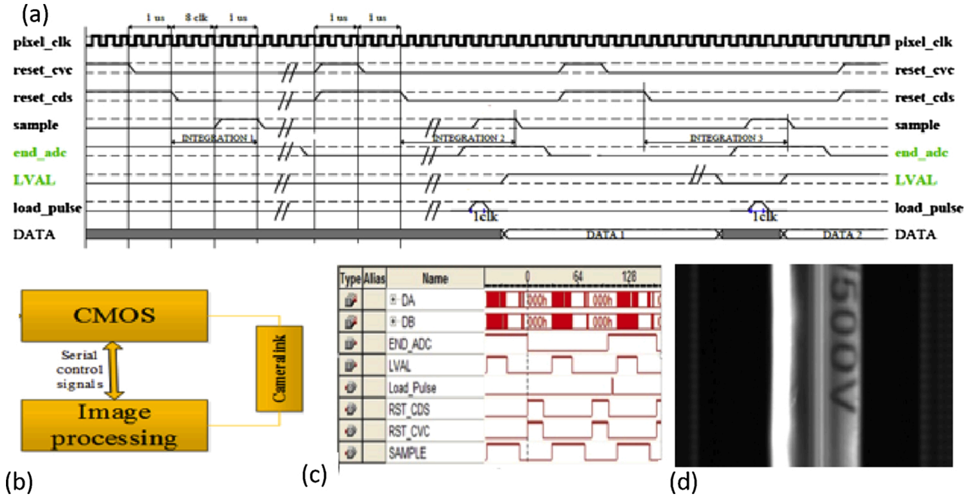


**Fig. 2.** (a) The timing diagram of DR-2k-7lcc, data from the CMOS can be read out when there is a load_puse signal each time; (b) Structure of the system, the control signal is sent from the FPGA to CMOS by serial wires, while data received by the FPGA is transferred by CameraLink wire; (c) The real-time process of imaging system; (d) Original real-time image.

receive data onto CMOS camera by the SPI and CameraLink respectively, as shown in Fig. 2(b).

QUARTUSIIfrom Altera Corporation is used to realize the modules of FPGA processing board. Signal Tap II, which is a simulation tool of QUARTUS, is used to test whether the signals in the FPGA match with the timing diagram or not, as shown in Fig. 2(c). With the help of functional simulation, the specific components of the RTL (Register Transfer Level) simulation can be realized, which can verify the feasibility of the system. After the initialization of CMOS linear camera, an experiment was made to verify the camera system. A

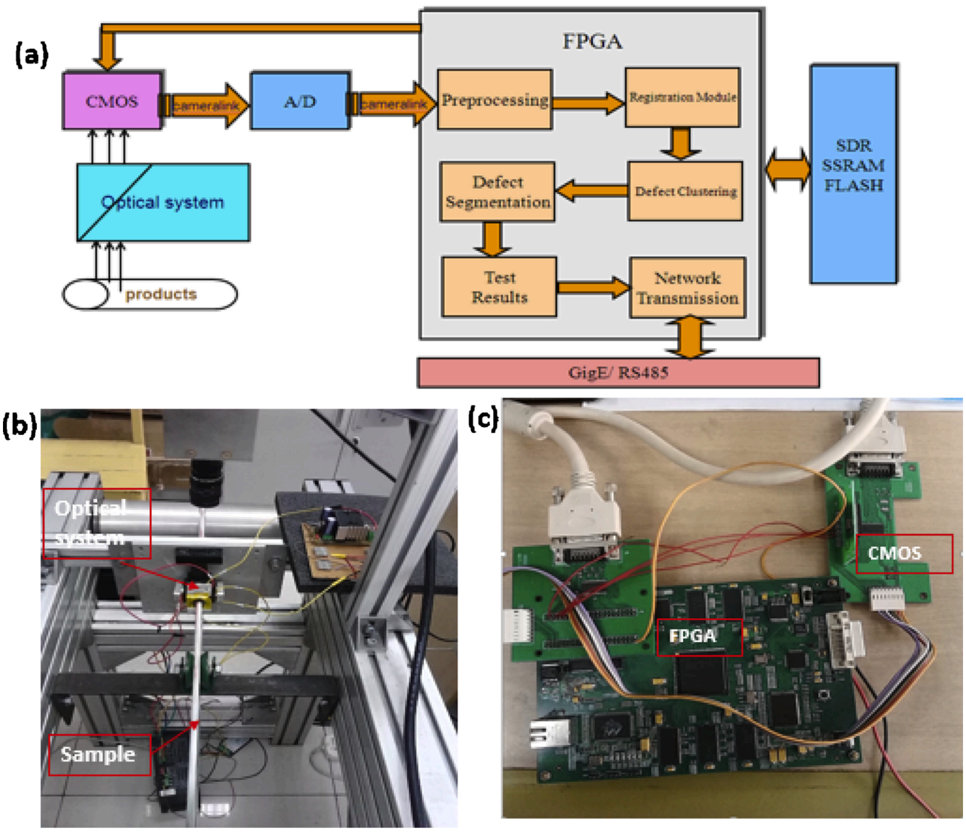


**Fig. 3.** (a) Schematic of the FPGA based detecting system; (b) Experiment platform; (c) Main board and CMOS driven board.

real-time picture was captured by the camera and received by the FPGA, then displayed on a screen of VGA (Video Graphic Array) interface, as shown in Fig. 2(d).

### 2.3. FPGA based image processing system

In order to realize on-line inspection, FPGA has been selected as an embedded image processing board. The whole system is as follows: Fig. 3(a) is the schematic of FPGA based inspection system. The curved surface information on products is extracted by a designed optical system and imaged on a line scan CMOS camera. The CMOS camera is driven and controlled by the FPGA based processing platform through the SPI link. The original imaging data is transferred to the FPGA through CameraLink wires. The line scan data is then organized as a frame of image, and then preprocessing to denoise and improve the quality of an extracted image. Then, the defects of extracted image are obtained by subtracting from a standard product image, and related image processing modules are used according to the specific applications. The information about related product images is stored into a flash card, and the control orders for the processing machine are sent through GigE or RS484 channels. Fig. 3(b) is the FPGA based real-time inspection system for curved surfaces. It is constructed by three parts: (1) Sample part. A stepper motor is used to drive the plastic rod sample with a desired speed. (2) Optical system. A designed optical imaging system is used to extract curved surface information with high fidelity. (3) The FPGA based control and processing board. As shown in Fig. 3(c), the FPGA based inspection platform is used to control the camera and process the related images.

## 3. Experimental result and analysis

The curved surface information was collected by the optical system, and then acquired by CMOS camera as inspection information. FPGA based vision system is used to acquire information on the curved objects and detect its flaws. Image processing board is used to recognize different information. Image processing procedures includes image preprocessing, image registration and defect segmentation. During the experiment, a plastic rod driven by a stepper motor was used to simulate the high speed movement. The rod sample was moved with speed of 12.8 m/s, and the required surface defect inspection accuracy is 0.2 mm. Thus, in order to capture the moving samples without losing details, the linear scan rate of the sensor should be faster than feeding speed of rod sample (64 kHz). The line scan sensor has 2048 pixels, and the size of each pixel is 7um × 7um. As the speed of the rod sample can reach to 12.8 m/s and the diameter of the curved surface rod sample is 7.8 mm, the semi-perimeter of the curved surface width can be calculated as 12.56 mm. In order to effectively detect tiny defects (0.2 mm × 0.2 mm), sampling interval $\Delta a$ should be less than or equal to 0.02 mm. The minimum number of required line scan CMOS pixels ($N_p \geq 64$) is determined by the curved surface semi-perimeter $L_1$ and the minimum sampling interval $\Delta a$, the relationship is as follows:

$$N_p \geq L_1 / a \tag{1}$$

Also, the total pixels of the line scan CMOS ($N_0 = 2048$) should be larger than the minimum required pixels, as shown in Eq. (2):

$$N_0 > N_p \tag{2}$$

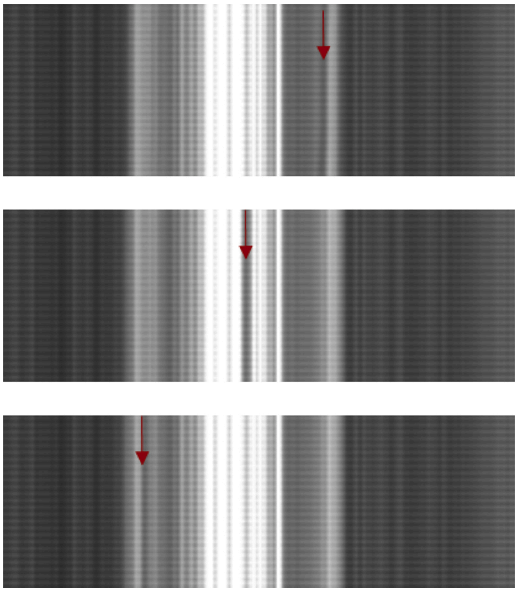

**Fig. 4.** Maximum imaging range experiment with black marked line.

The line sampling frequency of the line scan CMOS is determined by the longitudinal speed of product v and the minimum sampling interval Δa, which should satisfy the equation:

$$f \geq \frac{v}{\Delta a} = 12.8\,(m/s) \,/\, 0.2\,(mm) = 64\,kHz \tag{3}$$

### 3.1. Observing angle calculation

With the optical setup, a 180 degree observing angle is supposed to be obtained. A line mark scanning experiment had been applied to verify the real observing angle. The experiment is shown as follows: a plastic rod with a diameter of 7.8 mm was selected to pass through the cylindrical inspection tube. A straight black line mark was drawn along the axis direction of the plastic rod. When rotating the plastic rod, the limitation of rod can be seen from left to right by the black marked, as shown in Fig. 4. The red arrow indicated the black line mark moved from the right end to the left end. The perimeter length of the plastic rod was fixed to be: $L_2 = 7.8$ mm x $\pi = 24.5$ mm. So the observing angle for one camera is:

$$\theta = \frac{d}{L_2} \times 360^0, \tag{4}$$

where d is the black mark line moving distance, $L_2$ is the perimeter of the plastic rod, and θ is the observing angle of the camera.

During the black mark line moved from the right to the left side, the two ends of the marked area, which can be detected by camera, had been recorded. Then, the curved film attached on the plastic rod was flattened, and the distance between the two ends of the paper was measured as 11 mm. Thus, the observing angle can be calculated as 161.6 degrees, according to Eq. (4). The observing angle is smaller than 180 degrees, since there is an optical path deviation generated by lens mismatch and mechanical position. Also, the position of the imaging focal point affects the maximum imaging range.

### 3.2. Curved surface image acquisition

After acquiring the original curved surface image, image processing module should be used to extract the defects information of the curved surface on production line. In the process of producing curved surface paper, a variety of external factors result in different kinds of defects, especially black spots, dust, scratch, drape and so on. Due to the effects of industrial field environment, the curved surface paper image captured from line scan camera contains noises. Therefore, image filtering should be done for the curved surface image, and then the edge of the defect image can be detected by image processing. As the setup had not been assembled to the curved surface production line yet, a plastic rod has been used to simulate the initial experiment. An original image of the plastic rod has been taken from the CMOS camera as shown in Fig. 5(a). Then, the surface of the rod has been denoised with mediate filtering and extracted by a defined region of interest (ROI), and the followed processing algorithms will focus on this area, as shown in Fig. 5(b). Three designed drawbacks had been used for real-time inspecting: a black spot drawback had been designed on the image; a white scrub had been drawn on the image; and a black spot drawback and a white scrub had been set on the image, as in shown in Fig. 6(a)–(c).

### 3.3. Curved surface image inspecting

The original image with drawbacks of black spot and white scrub is shown in Fig. 7(a). To extract feature information, firstly the targeted image was handled with moving average of image threshold, and then eliminated or alleviated the residual printed text with morphological opening operation. Finally, removing the region of overexposure and the inspecting results can be derived. Image threshold segmentation is intuitive, easy to implement and fast to calculate. To reduce illumination bias, the moving average of image threshold is used to realize the image segment. This method is based on the moving average of the scanned rows of an image. The scan is performed line by line in a zigzag pattern. Assuming the grayscale of the points encountered in the scanning sequence in step k+1 is recorded as $z_{k+1}$. The average grayscale at this new point is given by the following equation:

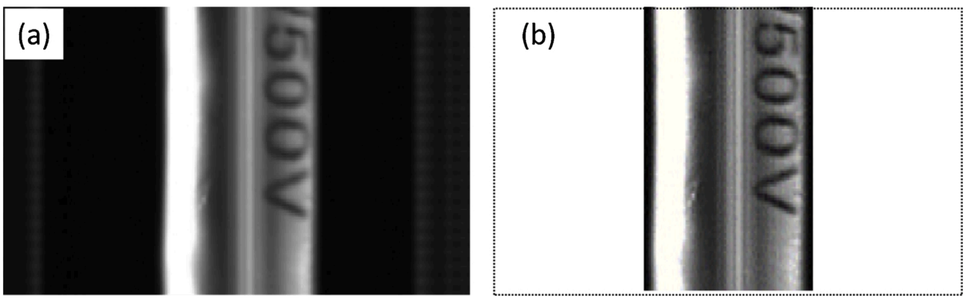


**Fig. 5.** (a) Original image; (b) The ROI and mediate filtering.

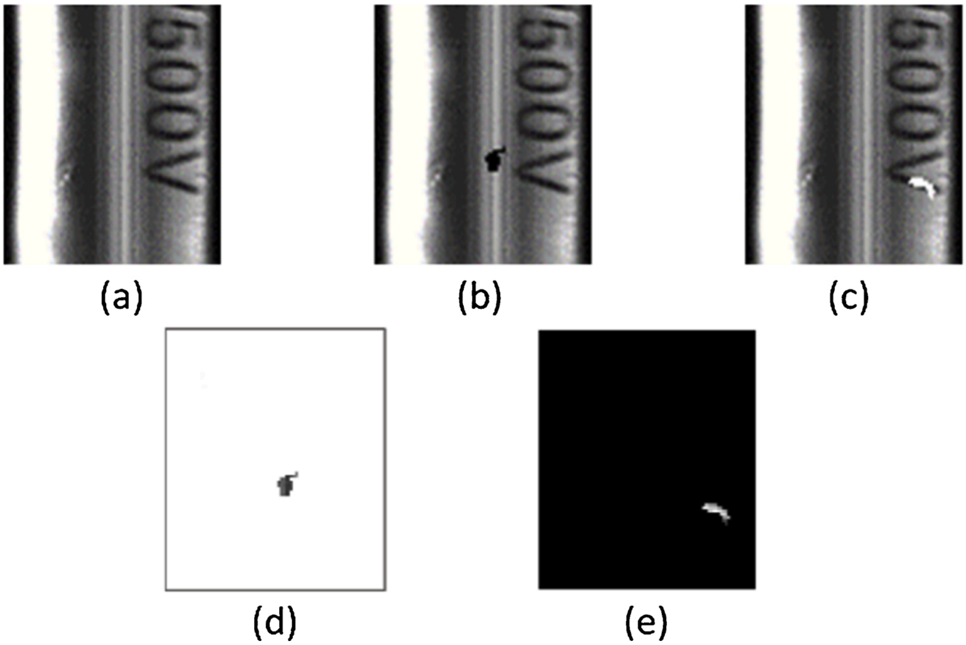


**Fig. 6.** (a) Template image; (b) Image with black spot draw back; (c) Image with scrub; (d) Black spot defect; (e) White scrub defect.

$$m(k+1) = \frac{1}{n}\sum_{i=k+2-n}^{k+1} z_i = m(k) + \frac{1}{n}(z_{k+1} - z_{k-n}), \tag{5}$$

where n is the number of points used to calculate the average, and $m(1) = z_1/n$. Then the image is divided into two parts:

$$g(x,y) = \begin{cases} 1, f(x,y) > T_{xy} \\ 0, f(x,y) \le T_{xy} \end{cases}, \tag{6}$$

where f(x, y) is the original image. $T_{xy}$ is variable local threshold and can be obtained by the following equation:

$$T_{xy} = bm_{xy}, \tag{7}$$

where $m_{xy}$ is the pixel set contained in the field centered on coordinate (x, y) in an image.

Each pixel is assigned to the target region or the background area, thus generating a corresponding binary image. According to experiments, setting $n = 20$, $b = 0.5$, the binarization of image is shown in Fig. 7(b). There is still residual printed text after most background information has been removed from the image segmented. Because the residual will affect the analysis of the defects feather, the image needs to deduct the residual with morphological opening operation. The image after deducted the residual is shown in Fig. 7(c), and the drawbacks of black spot and white scrub can be extracted completely. As there is still region of overexposure remained, morphological opening operation had been used to eliminate the overexposure area as shown in Fig. 7(d). Finally, the drawbacks on the curved surface can be extracted out, and it can be subsequently applied to various curved surface inspection areas.

## 4. Discussion

In this paper, a vision based real-time curved surface inspection system has been designed and manufactured. In this platform, a novel optical system has been developed to capture the outline appearance of the curved surface, and a line scan camera with the FPGA based processing board has been used to process the acquired image. This paper briefly introduces the working principle of CMOS imaging sensor and then presents a newly designed FPGA module which can initialize CMOS image sensor. CMOS image sensor controller programmed by Verilog hardware description language. According to the simulations and hardware circuit tested, CMOS image sensor controller has been implemented successfully. CMOS image sensor controller presented in this paper has great practical value for image processing and real-time inspecting areas. Image processing algorithms have been proposed, and initial defect inspection experiments has been done with plastic rods. The drawbacks of black spot and white scrub can be derived correctly. In the future, the real-time vision system can be realized in various surface inspection scenarios.

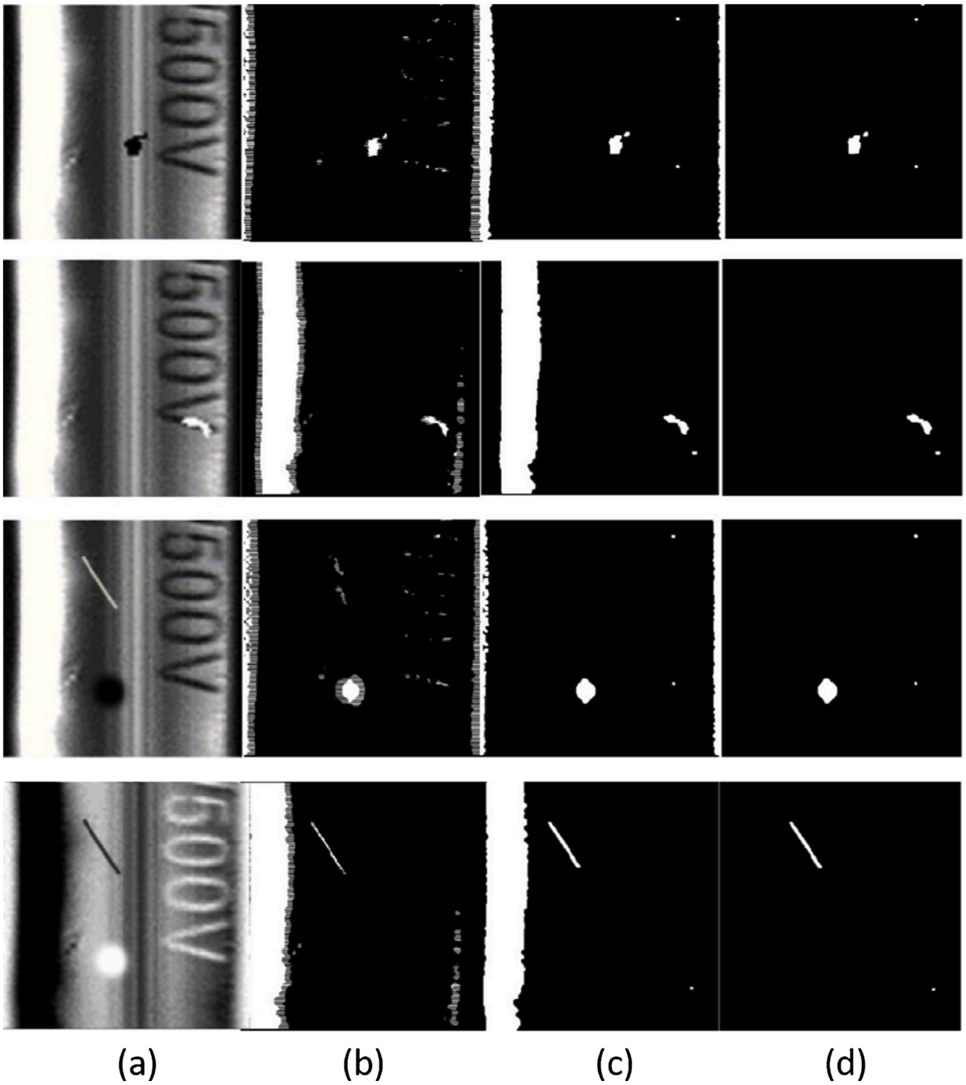


**Fig. 7.** (a) Original image; (b) Binary image obtained as a result of the moving average of image threshold ($n = 20$, $b = 0.5$), (c) Image after morphological opening operation, (d) Image after removing the region of overexposure.

## Impact statement

Surface quality plays an important role in inspection lines. We believe that three aspects of this manuscript will make it interesting to general readers of your journal. Firstly, a novel imaging device combined with FPGA based processing platform had been designed, which can be used to detect and analyze curved surface defects for vision inspection.

Secondly, the optical imaging part was made by an optical device which can be used to collect curved surface features without anamorphose.

Thirdly, inspecting experiments had been tested with an inspection accuracy of 0.2 mm × 0.2 mm which satisfied a 12 m/s real time vision inspection line, and research result can be subsequently applied to various surface inspection areas.

## Declaration of Competing Interest

Authors declare that they have no financial and personal relationships with other people or organizations that can inappropriately influence our work, there is no professional or other personal interest of any nature or kind in any product, service and company that could be construed as influencing the position presented in, or the review of, the manuscript entitled.

## Acknowledgments

This research was funded by the National Natural Science Foundation of China (51805194), Research Startup Project for New Teachers (2662020GXQD001) China Postdoctoral Science Foundation (2017M622411), and Hubei province postdoctoral Foundation (2017G13). The authors acknowledge the support from Flexible Electronics Research Center of HUST and HUST Analytical & Testing Center for providing experiment facilities.

## References

[1] G. Suh, Y.J. Cha, Deep faster R-CNN-based automated inspection and localization of multiple types of damage, in: Sensors and Smart Structures Technologies for Civil, Mechanical, and Aerospace Systems 2018, International Society for Optics and Photonics, 2018, 10598: 105980T.
[2] Jong Pil Yun, et al., Vision-based surface defect inspection for thick steel plates, Opt. Eng. 56 (5) (2017), 053108.
[3] A. Delgado, J. de Brito, J.D. Silvestre, Inspection and diagnosis system for wood flooring, J. Perform. Constr. Facil. 27 (5) (2013) 564–574.
[4] Q.U. Yongdong, et al., The Application of Image Processing Techniques in Analysis of Cigarette Packets Surface Defects, CCIT, 2014.
[5] T. Dawood, Z. Zhu, T. Zayed, Machine vision-based model for spalling inspection and quantification in subway networks, Autom. Constr. 81 (2017) 149–160.
[6] Oleksandr Semeniuta, Sebastian Dransfeld, Petter Falkman, Vision-based robotic system for picking and inspection of small automotive components, in: IEEE International Conference on Automation Science and Engineering (CASE), IEEE, 2016, 2016.
[7] Mehmet Baygin, et al., Machine vision based defect detection approach using image processing, in: International Artificial Intelligence and Data Processing Symposium (IDAP), IEEE, 2017, 2017.
[8] Shumian Chen, et al., Colored rice quality inspection system using machine vision, J. Cereal Sci. 88 (2019) 87–95.
[9] Jinjiang Wang, Peilun Fu, Robert X. Gao, Machine vision intelligence for product defect inspection based on deep learning and Hough transform, J. Manuf. Syst. 51 (2019) 52–60.
[10] Pablo Martinez, Mohamed Al-Hussein, Rafiq Ahmad, Intelligent vision-based online inspection system of screw-fastening operations in light-gauge steel frame manufacturing, Int. J. Adv. Manuf. Technol. 109 (3) (2020) 645–657.
[11] Sergio Cubero, Nuria Aleixos, et al., Advances in machine vision applications for automatic inspection and quality evaluation of fruits and vegetables, Food Bioproc. 4 (2011) 487–504.
[12] Mostafa Abdelrahman, et al., Flaw detection in powder bed fusion using optical imaging, Addit. Manuf. 15 (2017) 1–11.
[13] Aníbal Concha-Meyer, et al., Volume estimation of strawberries, mushrooms, and tomatoes with a machine vision system, Int. J. Food Prop. 21 (1) (2018) 1867–1874.
[14] Francisco Fons, Mariano Fons, Enrique Cantó, Run-time self-reconfigurable 2D convolver for adaptive image processing, Microelectron. J. 42 (1) (2011) 204–217.
[15] Z. Xing, Y. Chen, X. Wang, et al., Online inspection system for wheel-set size of rail vehicle based on 2D laser displacement sensors, Optik 127 (4) (2016) 1695–1702.
[16] Tomasz Kryjak, Mateusz Komorkiewicz, Marek Gorgon, Real-time hardware–software embedded vision system for ITS smart camera implemented in Zynq SoC, J. Real. Image Process. 15 (1) (2018) 123–159.
[17] Patryk Fraczek, Andre Mora, Tomasz Kryjak, Embedded vision system for automated drone landing site detection, in: International Conference on Computer Vision and Graphics, Springer, Cham, 2018.
[18] Naoki Uchiyama, et al., Optimal motion trajectory generation and real-time trajectory modification for an industrial robot working in a rectangular space, J. Syst. Des. Dyn. 7 (3) (2013) 278–292.
[19] S.T. Oh, J.H. You, Y.K. Kim, FPGA acceleration of bolt inspection algorithm for a high-speed embedded machine vision system (ICCAS 2019), in: 2019 19th International Conference on Control, Automation and Systems (ICCAS), IEEE, 2019, pp. 1070–1073.
[20] I. Vido, I. Škorić, D. Mitrović, et al., Automotive vision grabber: FPGA design, cameras and data transfer over PCIe, in: 2019 Zooming Innovation in Consumer Technologies Conference (ZINC), IEEE, 2019, pp. 103–108.
[21] M.D. Raj, I. Gogul, M. Thangaraja, et al., Static gesture recognition based precise positioning of 5-DOF robotic arm using FPGA, in: 2017 Trends in Industrial Measurement and Automation (TIMA), IEEE, 2017, pp. 1–6.
[22] Lucas F.S. Cambuim, et al., An FPGA-based real-time occlusion robust stereo vision system using semi-global matching, J. Real. Image Process. 17 (5) (2020) 1447–1468.
[23] S. Nadeem, Nadeem Abbas, M.Y. Malik, Inspection of hybrid based nanofluid flow over a curved surface, Comput. Methods Programs Biomed. 189 (2020), 105193.
[24] Pengfei Zhang, et al., Simulation of the illuminating scene designed for curved surface defect optical inspection, in: International Society for Optics and PhotonicsSixth International Conference on Optical and Photonic Engineering (icOPEN 2018), Vol. 10827, 2018.
[25] Ailin Liu, Jinjin Zhang, Baoping Guo, Geometric distortion correction for streak camera imaging, J. Electron. Imaging 28 (3) (2019), 033023.
[26] F.E. Sahin, A.R. Tanguay, Distortion optimization for wide-angle computational cameras, Opt. Express 26 (5) (2018) 5478–5487.
[27] Anding Li, Youping Chen, Jingming Xie, Short-time Fourier transform method for online glass ream inspection, Opt. Eng. 55 (8) (2016), 083109.
[28] Heejoo Choi, et al., Modulated dark-field phasing detection for automatic optical inspection, Opt. Eng. 58 (9) (2019), 092603.
[29] Cong Liu, et al., Short-working-distance optical imaging system and method for surface detection of underwater structures, Sci. China Technol. Sci. 61 (5) (2018) 774–781.